Experimental Determination of the Particle Dynamics into a Rotating Tube

Francesco Desogus*, Renzo Carta

University of Cagliari – Department of Mechanical, Chemical and Material Engineering – Piazza d'Armi, 09123 Cagliari, Italy
f.desogus@dimcm.unica.it

This paper reports the procedure for analysing the biomass powder bed characteristics realized in an experimental pyrolysis reactor. The reaction apparatus is made of a quartz tube which can rotate, horizontally or slightly inclined, with different speeds. Depending on the tube inclination and rotation, different motion conditions (regime, hold-up, residence time and advancing rate) are possible; also the particle characteristics (nature, shape and size, humidity) and the flow rate affect the bed behaviour. After taking some pictures of the bed from the discharge side, they can be analysed by means of the geometry rules; this procedure is here described. In this way the bed profile can be obtained, and this information can be used to calculate the parameters of a proper model, already developed. The methodology here presented will be used in the future to find data to be used in the development of a whole pyrolysis process model including also heat exchange, gas fluid dynamics and pyrolysis reaction kinetics.

1. Introduction

Rotating drums represent a kind of device that is commonly used in industrial processing applications involving solids, particularly when a strict contact between the solid and a gas phase is needed. Examples of such operations are mixing, drying, milling, coating, granulation, grinding, calcination, and cement manufacturing. It has been demonstrated that rotating reactors can be used also in pyrolysis processing, in a wide variety of operating conditions and with many kinds of feed, like sewage sludge (Pedroza et al., 2014) or agricultural biomass (Desogus et al., 2016). Pyrolysis can be successfully operated with different kinds of organic wastes, even mixed, like biomass and plastics (Oyedun et al., 2014) or peat and petroleum containing waste (Kosivtsov et al., 2015), and revealed to present many advantages with respect to alternative processes (mainly combustion and gasification) in the treatment of solid wastes: lower dioxin and furan emissions (the reaction environment is reducing, with little amounts of oxidizing agents), lower consumption of fossil fuels (in some cases the products can be burnt for the reactor heating, making the whole process autonomous from the energy point of view), higher flexibility in the characteristics of the material to be treated (Descoins et al., 2005). This kind of process could contribute to the reduction of the global CO_2 emissions, particularly in agriculture, if it is considered that "Agriculture, forestry and other land use" economic sector is responsible for 24 % of the total emission (Wan Alwi et al., 2016). However, as pointed out by Lim et al. (2016), the product characteristics change depending on the feedstock ones, and need to be predicted. Furthermore, Descoins et al. (2005) also highlight that to carry on a pyrolysis process in a rotary kiln needs a specific knowledge of the behaviour of this apparatus, considering both the solid dynamics which happen inside the tube and the influence of the operating parameters on the product yields and characteristics. For these reasons, a process model should take into account all the happening phenomena together and their interactions: solid motion dynamics, heat transfer between walls and solid phase, heat transfer between particles, heat transfer between solid and gas phase, gas phase fluid dynamics, and reaction kinetics. About the first aspect, many techniques have been used to determine the behaviour of granular solids inside rotating cylinders, and are described in the scientific literature: Magnetic Resonance Imaging (Kawaguchi, 2010), Positron Emission Particle Tracking (Ingram et al., 2005), fibre optics probes (Boateng and Barr, 1997), Particle Image Velocimetry and Particle

Tracking Velocimetry (Mellmann et al., 2004), and Radioactive Particle Tracking (Alizadeh et al., 2013). Unfortunately, as Huang et al. (2013) report, these techniques are often limited in the possible observations and are not always suitable in the case of ordinary and experimental processing. Moreover, only few studies have been focused on non-spherical particles (normally obtained by biomass mincing), and they have been conducted only with some particular kinds of particles. From this, the extension to different systems is difficult or impossible. Thus, the present work presents the development of a technique that revealed to be very useful in the study of the solid particles advancing along the reactor axis while working, and that can be used also in other systems, when information about the bed profile are needed. The work was developed by means of a laboratory reactor, the description of which will be given in the next section.

2. Materials and methods

2.1 Materials

The methodology proposed in this article has been developed and tested by means of a laboratory experimental structure that is used to perform pyrolysis processing of minced biomass. The main part is a commercial laboratory scale rotating furnace produced by Nabertherm® (rotary tube furnace for continuous processes, model RSR 120-750/11, see Figure 1(a)). The tube furnace is a quartz cylinder with a total length of 179 cm, an inner diameter of 10 cm and an outer one of 10.6 cm. The working tube can rotate, by means of an adjustable electric drive, with a rotational speed ranging between 1.33 and 30 rounds/min. The solid particles to be fed to the reactor are at first charged into a filling funnel, from which the particles are carried by a feed screw; the screw rotation (thus, the biomass flow rate) is made by another adjustable electric drive. A blade system, positioned at the inlet of the quartz tube, improves the particles blending and conveyance in the tube. At the end of the cylinder, the out coming particles are collected in a bottle. The working tube can be sloped through two hydraulic pistons positioned in the inlet part, and the tilt angle measure is provided by a digital display. The apparatus is also equipped with a gas supply system which is used during pyrolysis processing (it has not been used in the present study, which was conducted in atmospheric still air), and with a thermocouple system that is connected with a three-zone PLC temperature control.

The out coming biomass mass flow rate was continuously measured by positioning the collecting recipient on a technical balance (Ohaus®, Adventurer™ Pro AV 4102) which was connected to a computer by an USB interface and the weight data were collected, every 1 s, by the Ohaus® Data Acquisition Software.

The developed technique has been tested in the above described apparatus by using a particular kind of minced biomass, which is currently used for other studies about pyrolysis. The material was minced rape (B. napus L. v. oleifera) straw, collected from a previous variety field trial (Lazzeri et al., 2009) built at the "Mauro Deidda" experimental farm (University of Sassari, Department of Agriculture). The rape straw, after mincing by a shredder, was sieved to separate a powder with 1.5 mm of size. Then, the powder was dried at 120 °C for one hour (in the rotating furnace) and stored in sealed plastic containers until being used in the experiments.

2.2 Methods

The biomass bed profile was investigated in different experimental conditions as regards the three independent variables of the process: the biomass flow rate, the tube slope, and the cylinder rotating rate. The slope and the rotating rate were modified, respectively, by the hydraulic pistons and the drive already mentioned in section 2.1. The biomass flow rate was regulated by changing the rotating rate of the feed screw. The dependence of the flow rate on the rotating rate of the feed screw for the specific material here used was:

$$Q \left[\frac{cm^3}{min} \right] = 10,33 \cdot \omega_S \left[min^{-1} \right] \tag{1}$$

where Q is the particles flow rate and ω_S is the rotating speed of the feed screw; in Figure 1b the experimentally determined line is reported. The biomass, before being used, was minced, sieved and then dried, as described in section 2.1. After this, the biomass particles were charged in the filling funnel, and the screw and the tube were made rotating. When the particles arrived at the end of the tube, the weight acquisition began and its variations were monitored until had reduced to zero, that means working in the steady state with a constant biomass flow rate. Starting from that time, pictures of the bed were taken in the axial direction, from the bottom to the top, by a digital camera placed at the end of the cylinder (in Figure 2(a) some bed pictures are presented as an example). A sketch of the biomass route is reported in Figure 2(b).

Finally, the apparatus was stopped and the biomass still inside the cylinder was collected and its amount was measured for comparison purposes with the following image analysis results.
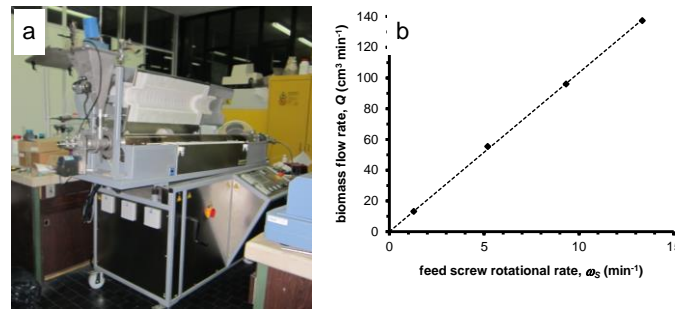
Figure 1: Picture of the experimental rotating kiln used in the present study (a). Characteristic curve, with the marked experimental points, of the dependence of the biomass flow rate on the feed screw rotational rate for the system here used (coefficient of determination for the regression line: 0.9995) (b).
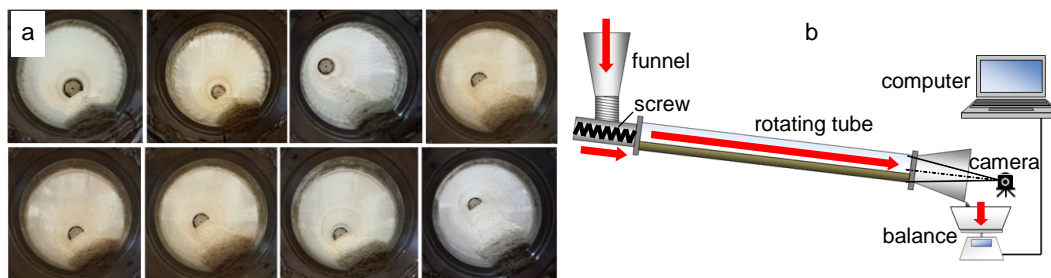

Figure 2: Example of pictures of the biomass bed taken from the bottom of the reactor in different working conditions (a). Sketch of the biomass route from the filling funnel, through the feed screw and the rotating tube, to the balance for the mass flow rate acquisition; the digital camera for the image acquisition is positioned at the bottom of the tube (b).
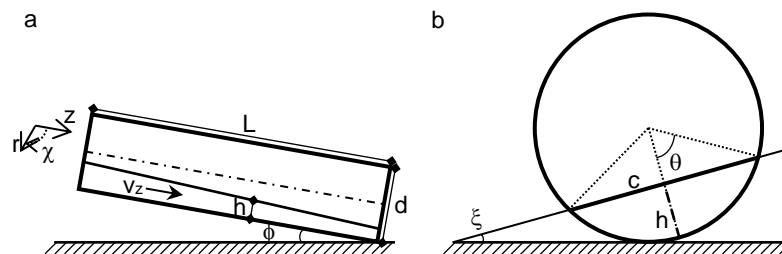

Figure 3: Longitudinal (a) and transverse (b) section of the minced biomass bed inside the inclined cylinder (z: axial coordinate; r: radial coordinate; χ: azimuthal coordinate; L: cylinder length; d: cylinder diameter; h: bed height; v_z: axial advancing rate of particles; φ: cylinder slope; θ: half of the central angle described by the bed in the transverse plane; c: chord of the circular segment occupied by the particles; ξ: angle between the chord and the horizontal plane).

3. Analysis development

In general terms, the system here studied (a biomass particle bed flowing through a rotating and inclined cylinder) can be represented in the scheme of Figure 3, in which the main parameters and notation are indicated.

For each image to be analysed (corresponding to a particular set of operating parameters to be investigated), the following procedure was carried out. It would be preferable to operate (as it has been done) on the electronic version of the image (even if with MS Office drawing tool), in such a way that the image could be resized (enlarged or restricted) as necessary to recognize all the particulars (the procedure is based on the human intervention for individuating the bed boundaries and all the other elements in the image), however it can be performed even on the printed image, if the printing quality and resolution are sufficient.
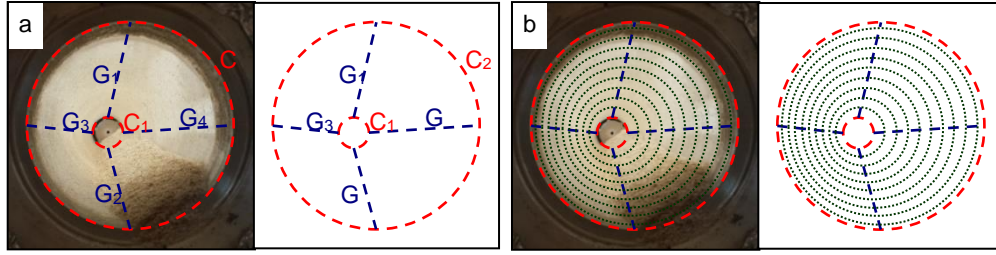
Figure 4: Graphical individuation of the top (circumference C_1) and of the bottom (circumference C_2) sections, in red; the highest (line G_1), lowest (line G_2), leftmost (line G_3) and rightmost (line G_4) generatrices are drawn in blue (a). Construction of internal circumferences (in green) (b).

3.1 Transverse section analysis

The first step consists in identifying the top (corresponding to the tube inlet) and the bottom (corresponding to the tube outlet) sections by drawing two circumferences overlapping the last visible feeding blade on background (top section, C_1 in Figure 4(a)) and the tube exit contour (bottom section, C_2 in Figure 4(a)). After this, four generatrices of the cylinder are traced passing for the highest (G_1 in Figure 4(a)), the lowest (G_2 in Figure 4(a), the leftmost (G_3 in Figure 4(a)) and the rightmost (G_4 in Figure 4(a)) points. The generatrices previously drawn make possible to build other circumferences, corresponding to internal sections, in a number equal to the number of desired measurements inside the cylinder, in fact all the most external points of the internal round sections are points of these generatrices. This step is represented in Figure 4(b). After this, the bed free surface must be individuated. To correctly do this, it should be considered that the bed shape becomes irregular near the blades at the inlet part of the tube and also just before the outlet section, caused by their disturbance effect. If the bed profile in these particular zones is of interest, they can be enlarged and studied in detail, otherwise they can be ignored and only the shape of the bed free surface in the internal part of the tube, where the profile is fully developed, can be considered, as shown in Figure 5(a).

Now, overlapping the constructions of Figures 4(b) and 5(a), the intersections between each internal section circumference (of Figure 4(b)) and the bed contours (of Figure 5(a)) give the extreme points of the chord for each section. In Figure 5(b) a particular of this construction is shown: for each section, the chord length (c), the bed depth (h), the central angle described by the bed in the transverse plane (2θ), and the angle between the chord and the horizontal plane (ξ) can be determined. It should be noted that, having the camera been positioned in such a way that the picture is taken perpendicularly to the transverse plane of the tube, the circumference, the chord and the bed height segments are all parallel to the page plane, and so all the dimensions on the picture are proportional to the real ones. As regards the angles θ and ξ, being all the linear dimensions on the picture proportional to the real ones, they are the same on the picture and in the real tube.

The last step is calculating the effective dimensions of the chord and of the bed height. Considering that they are proportional to c and h (dimensions on the picture), and that also the circumference diameter (d) can be obtained from the picture, the effective dimensions can be calculated by the following relationships:

$$c_{eff} = c \cdot \frac{d_{eff}}{d} \tag{2}$$

$$h_{eff} = h \cdot \frac{d_{eff}}{d} \tag{3}$$

In Eq(2) and Eq(3), c_{eff}, d_{eff} and h_{eff} are the effective segment lengths of, respectively, c, d and h.

Of course, the angle θ is also related to c and d (and to c_{eff} and d_{eff}) by the following geometrical relationship:

$$\theta = \arcsin\left(\frac{c}{d}\right) = \arcsin\left(\frac{c_{eff}}{d_{eff}}\right) \tag{4}$$

Furthermore, the following relationship between h (h_{eff}), d (d_{eff}) and θ exists for a circular segment:

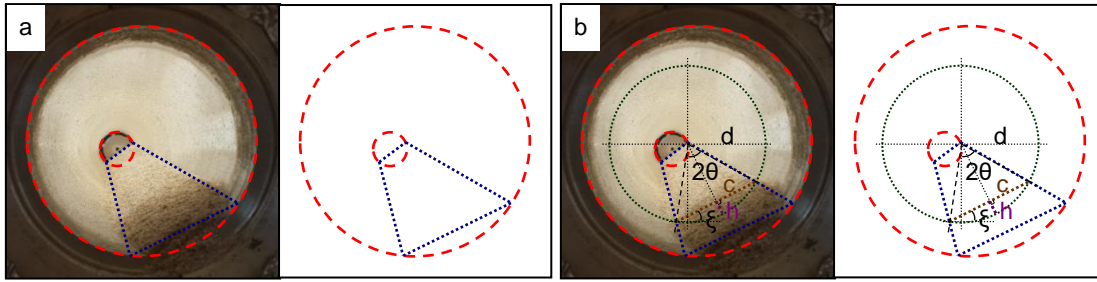$$h = \frac{d}{2} \cdot \left[1 - \cos(\theta)\right] \tag{5a}$$

Figure 5: Construction of the bed free surface (in blue) (a). Graphical individuation of the chord (c, in brown), the bed height (h, in violet), the circumference diameter (d), the central angle described by the bed in the transverse plane (2θ) and the angle between the chord and the horizontal plane (ξ) (b).

$$A_{eff} = \frac{1}{2} \cdot \left(\frac{d_{eff}}{2} \right)^2 \cdot \left[2\theta - \sin(2\theta) \right] \tag{6}$$

3.2 Axial dimension analysis

After having determined the chord length, the bed height and the angles θ (individuating the width of the bed) and ξ, to complete the information about the bed profile it is necessary to obtain the axial position for each transverse section previously considered, i.e. all the found parameters should be given as a function of z, being z the axial coordinate, starting from z_0 (z value at the inlet of the cylinder) to z_L (z value at the outlet of the cylinder). To do this, the perspective rules can be used in order to get this information from the two-dimensional images. With reference to Figure 6, after drawing the ground line (GL, arbitrarily positioned, for example tangent to the outlet section circumference) and the horizon line (HL, passing for the centre of the inlet section circumference), a "point of distance" (P) is positioned on the horizon line. From P, a projection (P-I) is traced, passing through the intersection (I) between the transverse section circumference and the cylinder lower generatrix (or any another), and prolonged until GL. The point of intersection between the projection and the ground line identifies on this a segment which is proportional to the axial distance. In fact, since I_T' and I_B' are fixed on the ground line, the axial position of I can be found through the following expression:
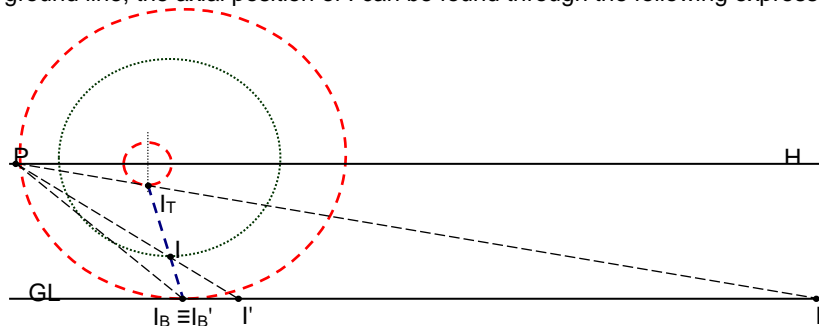

Figure 6: Perspective construction for determining the axial distance of the transverse planes. GL: ground line; HL: horizon line; P: point of distance; I: point of intersection between the transverse section circumference and the lower cylinder generatrix; I_T: point of intersection between the top (inlet) section circumference and the lower cylinder generatrix; I_B: point of intersection between the bottom (outlet) section circumference and the lower cylinder generatrix; I': point of intersection between the projection P-I and the ground line; I_T': point of intersection between the projection P-I_T and the ground line; I_B': point of intersection between the projection P-I_B and the ground line.

$$\left(\overline{I_T\text{-}I} \right)_{eff} = \left(\overline{I_T\text{-}I_B} \right)_{eff} \cdot \left(\overline{I_T'\text{-}I'} \right) \Big/ \left(\overline{I_T'\text{-}I_B'} \right) \tag{7}$$

As a consequence, in terms of the z coordinate, the distance from the top section can be expressed as:

$$z = z_0 + (z_L - z_0) \cdot \left(\overline{I_T\text{'-}I'} \right) \Big/ \left(\overline{I_T\text{'-}I_B'} \right) \tag{8}$$

4. Conclusions

The image analysis technique proposed in the present work makes possible to determine the bed profile into the rotating tubular reactor in different operating conditions. The main advantage is the possibility of obtaining this information by a non-invasive way and with high accuracy. The obtained data are the transverse section area of the bed, its depth and the angle between the bed free surface and the horizontal plane as a function of the axial coordinate. The methodology will be useful in the future study of the bed dynamic inside the rotating tube as a function of the operating conditions (biomass flow rate, cylinder slope and rotation rate) and will integrate the kinetic studies about pyrolysis, which will be conducted in parallel by the authors (Desogus and Carta, 2016).

Acknowledgments

Reference

Alizadeh E., Dubé O., Bertrand F., Chaouki J., 2013, Characterization of mixing and size segregation in a rotating drum by particle tracking method, AIChE J. 59, 1894-1905.

Boateng A.A., Barr P.V., 1997, Granular flow behaviour in the transverse plane of a partially filled rotating cylinder, J. Fluid. Mech. 330, 233-249.

Descoins N., Dirion J.-L., Howes T., 2005, Solid transport in a pyrolysis pilot-scale rotary kiln: preliminary results – stationary and dynamic results, Chem. Eng. Process. 44, 315-321.

Desogus F., Carta R., 2016, Setup of an experimental system to study the gas phase kinetics in pyrolysis processing, ECOS 2016 – 29th International Conference on Efficiency, Cost, Optimization, Simulation, and Environmental Impact of Energy Systems, 19-23 June 2016, Portorož (Slovenia).

Desogus F., Pili F., Carta R., 2016, Experimental study on the axial mass transport of minced biomass (rape straw) into a pyrolysis rotating reactor working in the slipping regime, Chem. Eng. Sci. 145, 80-89.

Huang A.-H., Kao W.-C., Kuo H.-P., 2013, Numerical studies of particle segregation in a rotating drum based on Eulerian continuum approach, Adv. Powder Technol. 24, 364-372.

Ingram A., Seville J.P.K., Parker D.J., Fan X., Forster R.G., 2005, Axial and radial dispersion in rolling mode rotating drums, Powder Technol. 158, 76-91.

Kawaguchi T., 2010, MRI measurement of granular flows and fluid–particle flows, Adv. Powder Technol. 21, 235-241.

Kosivtsov Y.Y., Chalov K.V., Lugovoy Y.V., Sulman E.M., Stepacheva A.A., 2015, Co-pyrolysis of peat and petroleum containing waste on Ni and Co containing catalysts, Chem. Eng. Trans. 45, 667-672.

Lazzeri L., D'Avino L., Mazzoncini M., Antichi D., Mosca G., Zanetti F., Del Gatto A., Pieri S., De Mastro G., Grassano N., Cosentino S., Copani V., Ledda L., Farci R., Bezzi G., Lazzari A., Dainelli R., Spugnoli P., 2009, On farm agronomic and first environmental evaluation of oil crops for sustainable bioenergy chains, Ital. J. Agron. 4, 171-180.

Lim C.H., Mohammed I.Y., Abakr Y.A., Kazi F.K., Yusup S., Lam H.L., 2016, Novel input-output prediction approach for biomass pyrolysis, J. Clean. Prod. 136, 51-61.

Mellmann J., Specht E., Liu X., 2004, Prediction of rolling bed motion in rotating cylinders, A.I.Ch.E. J. 50, 2783-2793.

Oyedun A.O., Gebreegziabher T., Ng D.K.S., Hui C.W., 2014, Mixed-waste pyrolysis of biomass and plastic waste – A modelling approach to reduce energy usage, Energy 75, 127-135.

Pedroza M.M., Sousa J.F., Vieira G.E.G., Bezerra M.B.D., 2014, Characterization of the products from the pyrolysis of sewage sludge in 1 kg/h rotating cylinder reactor, J. Anal. Appl. Pyrol. 105, 108-115.

Wan Alwi S.R., Klemeš J.J., Varbanov P.S., 2016, Cleaner energy planning, management and technologies: perspectives of supply-demand side and end-of-pipe management, J. Clean. Prod. 136, 1-13.